Published online 27 April 2007

Nucleic Acids Research, 2007, Vol. 35, No. 10 ***3355–3366***
doi:10.1093/nar/gkm190

Interplay between DNA *N*-glycosylases/AP lyases at multiply damaged sites and biological consequences

Grégory Éot-Houllier[1], Marta Gonera[1], Didier Gasparutto[2], Céline Giustranti[1] and Evelyne Sage[1,*]

[1]CNRS-IC UMR 2027, Institut Curie, Centre Universitaire, F-91405 Orsay, France and [2]Laboratoire ''Lésions des Acides Nucléiques''/Service de Chimie Inorganique et Biologique UMR E3 CEA-UJF/Département de Recherche Fondamentale sur la Matière Condensée, CEA-Grenoble, F-38054 Grenoble Cedex 9, France

Received February 2, 2007; Revised February 28, 2007; Accepted March 16, 2007

ABSTRACT

Evidence has emerged that repair of clustered DNA lesions may be compromised, possibly leading to the formation of double-strand breaks (DSB) and, thus, to deleterious events. The first repair event occurring at a multiply damaged site (MDS) is of major importance and will largely contribute to the hazardousness of MDS. Here, using protein extracts from wild type or hOGG1-overexpressing Chinese hamster ovary cells, we investigated the initial incision rate at base damage and the formation of repair intermediates in various complex MDS. These MDS comprise a 1 nt gap and 3–4 base damage, including 8-oxoguanine (oG) and 5-hydroxyuracil (hU). We report a hierarchy in base excision that mainly depends on the nature and the distribution of the damage. We also show that excision at both oG and hU, and consequently DSB formation, can be modulated by hOGG1 overexpression. Anyhow, for all the MDS analyzed, DSB formation is limited, due to impaired base excision. Interestingly, repair intermediates contain a short single-stranded region carrying a potentially mutagenic base damage. This *in vitro* study provides new insight into the processing of MDS and suggests that repair intermediates resulting from the processing of such MDS are rather mutagenic than toxic.

INTRODUCTION

Ionizing radiation produces a broad spectrum of lesions in DNA, including oxidized purines, oxidized/reduced pyrimidines, sites of base loss (AP sites), single-strand breaks (SSB), which are similar to those generated during oxidative metabolism. When found isolated, those lesions are efficiently and accurately repaired by the base excision repair (BER) pathway that is initiated by excision of damaged bases by specialized DNA *N*-glycosylases/AP lyases (1,2). There is evidence that those lesions can readily occur as clusters through energy deposition of ionizing radiation in nanometer volumes (3–7). A site of clustered lesions, also called multiply damaged site (MDS), consists of one or more damaged bases, AP sites or SSB closely spaced within 1–2 helix turns of DNA (3,5). Clustered lesions are still processed by the BER pathway. Due to the diversity and the proximity of damage comprised in an MDS, they are thought to be difficult to repair (8,9). There is a risk to generate double-strand breaks (DSB) as a result of accumulation of SSB as repair intermediates.

The *in vitro* repair efficiency of clustered lesions by pro- and eukaryote BER proteins or by cell extracts have been exhaustively examined mainly using oligonucleotides engineered to contain two closely opposed lesions. These studies have established that the excision efficiency of a lesion within a cluster depends on the type of lesions and on their position relative to each other (10–16, 8 for review). For instance, significant inhibition of base excision and incision at an AP site occurs if a SSB or another AP site is present 1–5 bp away in the 3′ or 5′ direction on the opposite strand, whereas the presence of a second base damage has little or no effect on the excision of a 8-oxo-7,8-dihydroguanine (oG) or 5,6-dihydrothymine. The repair of SSB, that involved short patch BER, was also retarded (17,18) or prevented when a SSB is terminated by a 3′oG (19). Inhibition of base excision should limit the formation of DSB in the processing of MDS. Studies in *Escherichia coli* and in mammalian cells also demonstrated that the repair of MDS is compromised and leads to mutations (20–22). Clustered lesions composed of two closely opposed uracil residues situated $\leq$7 bp apart were readily converted into DSB in *E. coli* but not in human cells (23,24). In accord with this, Dianov *et al.* (20) reported, in *E. coli*, a 10-fold more effective deletion induction in plasmid DNA with two opposed uracil residues located 12 bp apart than in DNA carrying a single uracil residue. Two-clustered oG did not

*To whom correspondence should be addressed. Tel: +33 1 6986 7187; Fax: +33 1 6986 9429; Email: Evelyne.Sage@curie.u-psud.fr

constitute a lethal event, but enhanced mutation frequency (mainly G to T transversion), relative to single lesion, and did not result in DSB or deletions in *E. coli* (21,25). Inactivation of the three major oxidative DNA *N*-glycosylases/AP lyases renders the *E. coli* triple mutant significantly more radioresistant than wild-type cells, likely due to a reduced formation of DSB at clustered lesion post-irradiation (26). Overexpressing either DNA *N*-glycosylases/AP lyases, hOGG1 or hNTH1, in human lymphoblastoid cells resulted in a significant increase in DSB which correlated with an elevated sensitivity to γ-rays and an enhanced mutation induction, whereas down-regulation of hOGG1 led to radioresistance and reduced DSB formation (27,28).

In a previous work (18), using human cell extracts and purified proteins, we explored the mechanism and efficiency of the different repair steps of a complex MDS, carrying four base damage and 1 nt gap distributed on both strands within 17 bp. We revealed a hierarchy in the processing of lesions within MDS, in particular at the base excision/incision step. Strong inhibition of oG excision was observed and attributed to the presence of both a 1 nt gap and an efficiently cleaved 5-hydroxyuracil (hU) located at 3 nt from oG on the opposite strand. We concluded that the hierarchy in excision of base damage within our MDS prevented DSB formation. Others established the influence of the nature, the positioning and the interlesion spacing of two closely opposed lesions on their processing (see above). Here, we investigated other parameters that control the first repair event at MDS to gain a better understanding of how MDS are processed. Using whole cell extracts from Chinese Hamster Ovary (CHO) cells overexpressing or not hOGG1, we analyzed the base excision rate in two similar complex MDS, except that in one of them oG and hU are in inverted position.

MATERIALS AND METHODS

DNA substrates

Unmodified oligonucleotides were purchased from Proligo-France and oligonucleotides carrying modified bases were synthesized as previously described (18). Various MDS constructs with different orientation and complexities were built, as depicted in Figure 1. Our most complex construct, MDS-1, comprises 4 oxidized bases within 17 bp, i.e. 8-oxoguanine (oG) and 8-oxoadenine (oA) separated by 7 nt on one strand, 5-hU and 5-formyluracil (fU) located on the other strand at 7 nt on either side of a 1 nt gap. Opposed lesions are positioned 3 bp apart. MDS-2 consists of the same construct except that oG and hU are in an inverted position and that oA was replaced by an adenine. SDS-oG and SDS-hU are simply damaged sites (SDS) used as control for single oG or hU, respectively. Oligonucleotides containing the lesion of interest (oG or hU) were 5′-^{32}P-end-labeled with [γ-^{32}P]-ATP (4500 Ci/mmol, ICN, Irvine, CA, USA) using T4 polynucleotide kinase (Invitrogen Life Technologies, Carlsbad, CA, USA) following instructions provided by the supplier. After removal of unincorporated nucleotides using a Probe Quant G-50 Micro Column (Amersham Pharmacia Biotech, Piscataway, NJ, USA), labeled oligonucleotides were hybridized, in 100 mM KCl, 10 mM Tris–HCl pH 7.8 and 1 mM EDTA, with a 1.8-fold excess of their respective complementary strand, by heating 5 min at 95°C and slow cooling to room temperature. The annealing efficiency was verified by migration of DNA duplexes on 12% native polyacrylamide gel. All but two double-stranded DNA substrates are 56 bp long (Figure 1).

Construction of stable CHO cell lines overexpressing hOgg1

Chinese hamster ovary AT3-2 cells were maintained in minimum essential medium-alpha (MEM-α) supplemented with 10% fetal calf serum, non-essentiel amino-acids (0.1 mM), penicillin (100 U/ml) and streptomycin (100 μg/ml). Transfections were performed with pPR65 (a generous gift from Dr P. Radicella, CEA/CNRS, Fontenay-aux-Roses, France), which allows expression of hOGG1 protein or with pcDNA3.1(−) (empty plasmid) as previously described (29). Two days post-transfection,

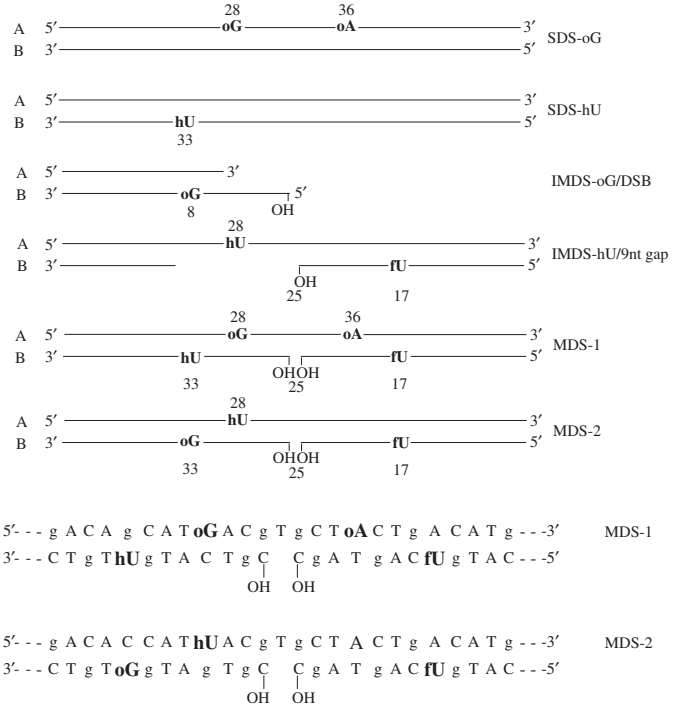

Figure 1. Schematic representation of damaged double-stranded DNA substrates. The oligonucleotides used to generate the DNA substrates were described previously (18). Substrates called simply damaged site (SDS) carry either oG and oA on strand A, or hU on strand B. Substrates named intermediary multiply damaged Sites (IMDS) carry either oG and oA on strand A and hU on strand B, or oG on strand B at 3 bp from a DSB, or hU on strand A and a 9 nt gap across. MDS-2 is equivalent to MDS-1 without oA and with oG and hU in inverted positions. IMDS-oG/DSB and IMDS-hU/9-nt gap are repair intermediate of MDS-2. The position of the lesions is relative to the 5′-end. Lesions located on the same strand are 7 nt apart and opposed lesions are separated by 3 bp. All duplexes are 56 bp long, except IMDS-oG/DSB and IMDS-hU/9-nt gap. The sequence of MDS-1 and MDS-2 around the damaged sites are depicted at the bottom of the figure, as example for all the other substrates.

cells were plated in 60 mm dishes in selective medium containing geneticin (G-418, 0.5 μg/ml final concentration). After 10 days, individual clones were randomly picked up, propagated in 24-well plates, and analyzed for hOGG1 expression and activity to cleave oG as described below. Among the 50 clones analyzed, we selected two clones of different hOGG1 overexpression level and oG repair activity, OGG1+ and OGG1++ and a control clone, CTR, derived from pcDNA 3.1(−)-transfected cells.

Determination of cytotoxicity and mutation frequency induced by γ-rays in hOgg1-overexpressing CHO cells

Exponentially growing CTR and hOgg1-overexpressing cells were irradiated with increasing dose of γ-rays using a ^{137}Cs source, at a dose rate of 2 Gy/min. To determine cell survival, cells were plated in triplicate in 60 mm dishes, and incubated in growth medium for a week following irradiation. For induced mutagenesis assay, mutants were selected at the *HPRT* locus. Briefly, cells were cultured in growth medium for 6 days after irradiation, to allow expression of mutant phenotype. Then, 10^7 cells were plated in twenty 100 mm dishes, at 5×10^5 cells per dish, in growth medium supplemented with G418 (final concentration 0.5 μg/ml). Following 2-h incubation, 6-thioguanine was added to each plate (final concentration 2.5 μg/ml) for selection. Aliquots of 100 cells in non-selective medium were also seeded in triplicate in 60 mm dishes to determine the plating efficiencies. After 2 weeks, colonies were washed in 0.9% NaCl, stained with a solution of 1% methylene blue prepared in 50% methanol and counted. Survival fractions correspond to the ratio of plating efficiencies of irradiated cells and unirradiated cells, and induced mutation frequencies were established as the number of mutant colonies in selective medium per surviving cells in non-selective medium.

Cleavage assay by whole protein cell extracts

Whole-cell extracts were prepared from CHO parental cells, CTR-transfected and hOgg1-overexpressing cells, as previously described (18), except that lysis buffer was at pH 7.5 and aliquots conserved at −80°C. The cleavage reactions (75 μl final volume) were performed at 37°C by mixing 1.5 pmol of labeled double-stranded oligonucleotides and 150 μg of cell extracts in incubation buffer (20 mM Tris–HCl pH 7.5, 100 mM NaCl, 0.8 mM EDTA, 8% glycerol). At indicated time, 10 μl aliquots mixed to 10 μl of 1% SDS/0.1 M EDTA, and 5 μl of proteinase K (4 mg/ml) were added. Following 1-h incubation at 37°C and phenol/chloroform extraction, samples were denatured 5 min at 95°C in denaturing stop solution (94% formamide, 0.1% bromophenol blue, 0.1% xylene cyanol and 10 mM EDTA pH 8) and then subjected to electrophoresis on a 12% denaturing polyacrylamide gel containing 7 M urea and 10% formamide in TBE 1× (89 mM Tris–HCl, 89 mM boric acid and 2 mM EDTA, pH 8.3). The presence of DSB was analyzed as described above but non-denaturing stop solution (75% glycerol, 0.25% bromophenol blue and 0.25% xylene cyanol) was added to the samples, which were then electrophoresed on a native 12% polyacrylamide gel in TBE buffer. The reaction products were visualized and quantified using a Molecular Dynamics Storm 840 PhosphorImager and ImageQuant software (Molecular Dynamics, Piscataway, NJ, USA). The cleavage efficiency was expressed as the percentage of the amount of labeled cleaved molecules to the total amount of labeled (cleaved plus uncleaved) molecules in a lane.

Western blot analysis

Fifty microgram of proteins cell extracts were mixed with SDS loading buffer 5× (250 mM Tris–HCl pH 6.8, 10% SDS, 50% glycerol, 5% 2-β-mercaptoethanol and 0.5% bromophenol blue) and separated on a 10% SDS-PAGE. After migration, the gel was transferred on a nitrocellulose membrane. The protein hOGG1 was detected using a polyclonal rabbit antibody against the whole protein (a gift from Dr Pablo Radicella).

Trapping assay

Duplex substrates (1 nM) were incubated for 20 min at 37°C with increasing amount of hOGG1 protein (0–400 nM, a gift from Dr P. Radicella) in 20 μl of reaction buffer (25 mM Tris–HCl pH 7.6, 2 mM EDTA) containing 50 mM $NaBH_4$. Reactions were stopped by adding 10 μl of SDS loading buffer 3× containing 40% formamide, heated 5 min at 95°C and submitted to a 10% SDS-PAGE containing 3.5 M urea. Then, gels were dried and reaction products were analyzed as described above.

RESULTS

The distribution and the nature of oxidative damage contributes, respectively, to base excision efficiency and hierarchy within MDS

The role of the position (5′ or 3′) and of the interlesion spacing on the excision efficiency of two closely opposed lesions by purified repair proteins or cell extracts has already been investigated (14–16). In a previous work, we focused on the mechanism and efficiency of the different steps in the repair of a complex MDS, called MDS-1 (18). In order to gain insight into the role of damage distribution on MDS processing, we built MDS-2 (Figure 1), carrying oG and hU at inverted position relatively to MDS-1. It is noteworthy that we failed to detect any cleavage at oA in MDS-1 (18). Therefore, oA was replaced by A in MDS-2 (Figure 1). DNA duplexes with a single modified base, oG or hU, were used as control. P^{32}-end labeled MDS-1, MDS-2 and control DNA duplexes were incubated for different periods of time with CHO protein extracts, and cleaved products analyzed on denaturing polyacrylamide gel. As with human cell extract (18), cleavage at oG was largely decreased in MDS-1, compared to SDS-oG (Figure 2A, B). This confirms the major inhibitory role of a 1 nt gap on excision of oG situated on the opposed strand that we and others have previously established (15). The cleavage at oG within MDS-2 or SDS-oG followed the same kinetics (Figure 2B), showing that neither the presence of hU, positioned 4 nt 5′ to oG

on the opposite strand, nor the presence of the 1 nt gap located 6 nt away on the same strand, influenced oG excision. Interestingly, in contrast to oG, hU was efficiently cleaved in all the configurations tested, including MDS-2 (Figure 2C). This demonstrates that, in marked contrast to oG excision, hU excision is not altered by the presence of a 1 nt gap positioned 4 nt away on the opposite strand. These data reveal that cleavage at oG is more affected by the surrounding than cleavage at hU. In a trapping assay using purified human OGG1 (hOGG1) protein (Figure 2D), we show that the binding of the protein or its DNA *N*-glycosylase activity is, indeed, impaired in the MDS-1 context. As expected, the binding of hOGG1 at oG within MDS-2 is very efficient.

The competition between different DNA *N*-glycosylase/lyase activities is likely to play a crucial role on the outcome of the attempted repair at MDS. In particular, the kinetics of recognition and excision of the modified bases within an MDS may be the driving force for the first repair event. The time-course cleavage of SDS-hU

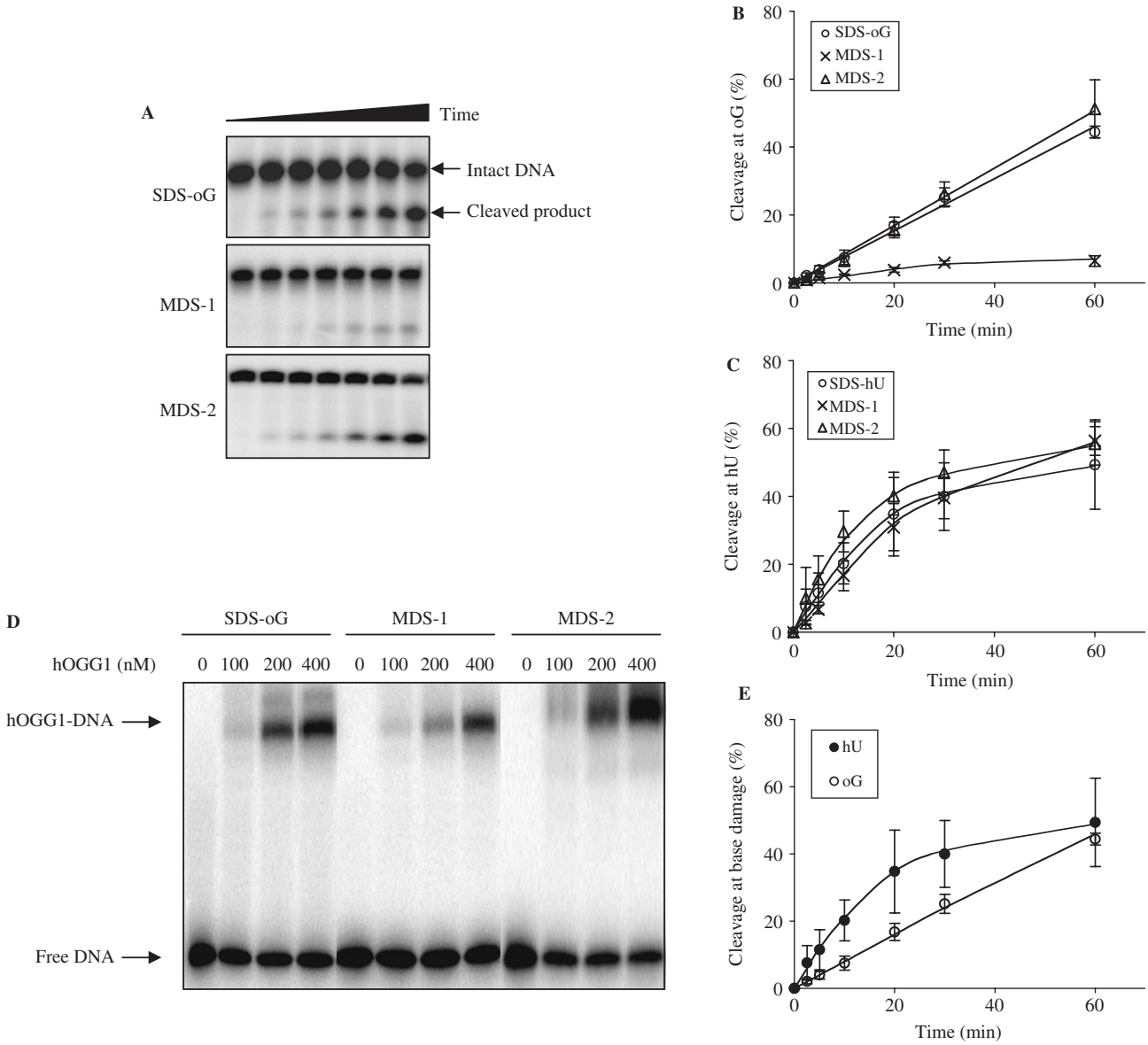

Figure 2. Influence of damage distribution on the cleavage efficiency at oG and hU within MDS by CHO whole-cell extracts. Here, 1.5 pmol of substrate, ^{32}P-labeled at the 5′end of the oligonucleotide containing the lesion of interest, were incubated at 37°C in the presence of 150 μg of extracts. Aliquots (200 fmol of substrate) were removed at various time (0–60 min) and reaction products were subjected to a 12% denaturing polyacrylamide gel. Cleavage efficiency at oG (**A** and **B**) and hU (**C**) as a function of incubation time is shown for SDS, MDS-1 and MDS-2, with standard deviation from at least three experiments. In (A), the products resulting from cleavage at oG are 28-nt long for SDS-oG and MDS-1, 7-nt long for MDS-2. The gel profiles of trapping assay (**D**) show the binding of hOGG1 protein to radiolabeled substrates SDS-oG, MDS-1 and MDS-2. SDS-oG and MDS-1 were labeled at the 5′-end of the oligonucleotide 56-mer containing oG and MDS-2 was labeled at the 5′ end of the oligonucleotide 31-mer carrying oG. 5′-End labeled duplexes were allowed to react with increasing amount of hOGG1 (0–400 nM) at 37°C for 20 min in buffer containing $NaBH_4$. The reaction products were separated using 10% SDS-PAGE containing 3.5 M urea. The reacted substrates were run on different gels. Kinetics of cleavage of SDS-oG at oG and SDS-hU at hU by cell extract are compared in (**E**).

and SDS-oG by the cell extract shown in Figure 2E reveals that duplex carrying a single base damage was more rapidly cleaved at hU than at oG. Moreover, hU was cleaved more rapidly than oG in all contexts tested, including MDS-2 (deduced from the initial slopes of curves shown in Figure 2B and C). The same hierarchy in the excision of hU and oG was thus observed for the two different arrangements of damage in MDS-1 and MDS-2. This highlights the importance of the nature of modified bases in the processing of MDS.

Overexpression of hOGG1 influences excision rate at oG as well as at hU within MDS, but it depends on damage distribution

To further investigate on the interplay between repair activities at MDS, we reasoned that the excision efficiency of a particular modified base depends on the amount of the DNA *N*-glycosylases/lyase specific to this lesion, which is actively present in the cell extract. We have shown that oG was mainly repaired by OGG1 in human cell extract (18), whereas hU might be a good substrate for NTH1, MUG1, NEIL1 and 2, and for APE1 to a lower extent (30–32). We observed that hU was cleaved about ten times more efficiently than oG in MDS-1 after an hour incubation with the extract (18; and Figure 2B). We asked if we could revert or modulate the repair hierarchy within MDS by modifying the level of OGG1 activity. To address this question, we overexpressed hOGG1 in CHO AT3-2 cells (see material and methods). We selected two clones overexpressing hOGG1, called OGG1+ and OGG1++ (Figure 3A), that differed in hOGG1 expression level, as revealed by western-blotting using anti-hOGG1 antibody (Figure 3A), and in their repair activity toward oG, using SDS-oG construct (Figure 3B). Indeed, OGG1+ and OGG1++ extract exhibited 1.6 and 4-fold increase in oG excision rate, respectively, in comparison with extract from the control clone CTR derived from transfection with empty plasmid (Figure 3B). Basal oG repair activity of CTR extract was superimposable to that of the extract from untransfected recipient CHO cells shown in Figure 2B. Those clones were also characterized on a biological point of view for their sensitivity to ionizing radiation. In a colony-forming assay, these cell lines exhibited the same sensitivity towards the cytotoxic effect of γ-rays (Figure 3C) as the parental cell line AT3-2 (data not shown). The mutation induction determined at the *HPRT* locus in OGG1++ cells was about 2.5-fold higher than in CTR cells, whereas it was only enhanced at a dose of 4 Gy in OGG1+ cell line (Figure 3D). Under our conditions, CHO cells overexpressing hOGG1 were sensitive to the mutagenic but not to the cytotoxic effect of ionizing radiation.

Using the same cell extracts, we then compared the excision rate (kinetics and amount of cleavage) at oG and hU as single lesions, using SDS-oG and SDS-hU substrates, respectively. As expected, SDS-hU was excised at about the same rate whatever was hOGG1 expression level (compare excision at hU in Figures 2C and 3E, F), since hU is not a substrate for OGG1 protein (30; and data not shown). The slope at the origin for the excision rate by OGG1+ extracts was 2-fold higher for hU than for oG (Figure 3E), it was 2.6-fold higher for excision rate at hU than at oG by control extract (Figure 2E). Meanwhile, the extent of cleavage at oG was higher than at hU after 1-h incubation with OGG1+ extract. Remarkably, the high level of hOGG1 protein in OGG1++ extract resulted in a slightly faster and more extensive cleavage (1.4-fold increase) at oG than at hU (Figure 3F). We thus obtained cell extracts harboring different capacity to cleave at oG, relatively to their ability to cleave at hU.

In order to determine whether or not the competition between *N*-glycosylases for their respective substrates could contribute to repair hierarchy within MDS, we analyzed the kinetics of cleavage at oG and hU within MDS-1 and MDS-2 by cell extracts from control and hOGG1-overexpressing cells. Using the MDS-1 substrate, we found that incision at hU was not modified by hOGG1 overexpression (Figure 4A). Cleavage rate at oG remained very low compared to hU in each extracts, although it was slightly increased in the OGG1++ cell extracts (Figure 4B). This result confirmed the strong inhibitory effect of a 1 nt gap on the excision of an oG positioned in close proximity on the opposed strand in the 3′ orientation. Therefore, in this configuration, the order of hU and oG cleavage remained unchanged in spite of conditions that favor oG processing. In contrast to MDS-1, overexpression of hOGG1 resulted in a large increase in the incision rate at oG within MDS-2 substrate (Figure 4D), but, unexpectedly, in a subtantial decrease of cleavage efficiency at hU (Figure 4C). Thus, the excision hierarchy at oG and hU within MDS-2 was controlled by the competition between the DNA *N*-glycosylases/lyases in the extracts. These data also reveal that, in the context of MDS, an elevated level of one DNA *N*-glycosylase/lyase may diminish the excision efficiency of a modified base, which is not substrate for this protein. In addition, this inhibitory effect is strongly correlated with the amount of overexpressed protein (Figure 4C).

In conclusion, our data demonstrate that, not only the positioning and nature of damage base within MDS are important for the processing of MDS, but also the relative amount of repair enzymes available in cells.

Consequences of hOGG1 overexpression on DSB formation during the processing of MDS

As excision rate of modified base in MDS did vary depending on the level of hOGG1 in the extracts, one could expect changes in DSB formation. To address this question, MDS-1 and MDS-2 were incubated with the different cell extracts, and reaction products were separated on native 12% polyacrylamide gels.

In the MDS-1 context, DSB formation results from cleavage at oG. Using duplex labeled on strand carrying oG, two populations of reaction products were observed, the band migrating as a 27 bp DNA duplex which corresponds to excision at oG only, and the band migrating as a 23 bp duplex which corresponds to excision at oG plus hU (Figure 5, lanes 2–4). Because of the low efficiency at incising at oG observed in Figure 4B, the extent

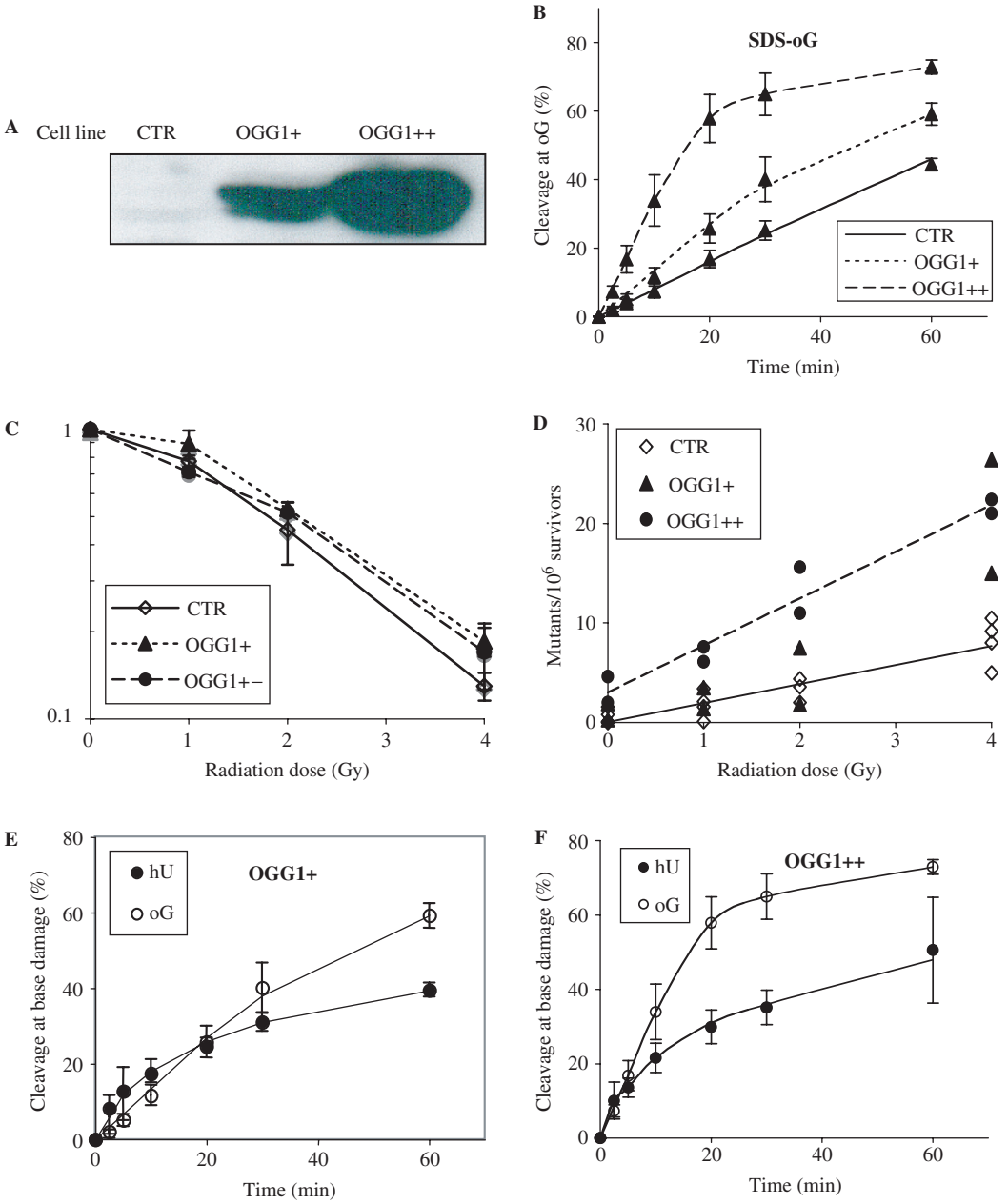

Figure 3. Characterization of CHO cell lines overexpressing hOGG1 protein. (**A**) Western blot analysis of hOGG1 protein levels in OGG1+ and OGG1++ transformants and in CTR cells transformed with empty plasmid. (**B**) DNA *N*-Glycosylase activities of hOGG1 measured by the cleavage of radiolabeled SDS-oG as a function of time, in CTR, OGG1+ and OGG1++ cell extracts. (**C**) Survival of CTR, OGG1+ and OGG1++ cells treated with 0, 1, 2 and 4 Gy of γ-rays. Cells were plated immediately after irradiation and survival fraction was established as the ability of irradiated cells to form colonies. Error bars represent standard deviation of 2–3 experiments. (**D**) Mutation frequencies at the *hprt* locus in CTR, OGG1+ and OGG1++ cells treated with 0, 1, 2 and 4 Gy of γ-rays. (**E**) and (**F**) Time course analysis (0–60 min) of cleavage efficiency at oG and hU in SDS-oG and SDS-hU respectively, by OGG1+ (E) and OGG1++ (F) extracts (mean of at least three independent experiments).

of DSB formation was also low and barely increased with enhanced hOGG1 expression level (6.5% for CTR extracts to 16% for OGG1++ extracts, Figure 5 compare lanes 2 and 6 to lanes 3–4 and 7–8, respectively). In fact, the major product observed resulted from cleavage at hU and poped out as a 7 nt single-stranded fragment, as can be seen when duplex is labeled on the strand carrying hU (Figure 5, lanes 6–8). As expected, overexpression of hOGG1 in OGG1+ and OGG1++ cells did not interfere with formation of this short single-stranded fragment. Altogether it indicates that MDS-1 processing predominantly resulted in a DNA duplex containing oG on a 9 nt single-stranded region, even in hOGG1-overexpressing cell extracts.

Using MDS-2 construct labeled on the strand carrying oG, a strong 27 bp band that corresponded to the DSB

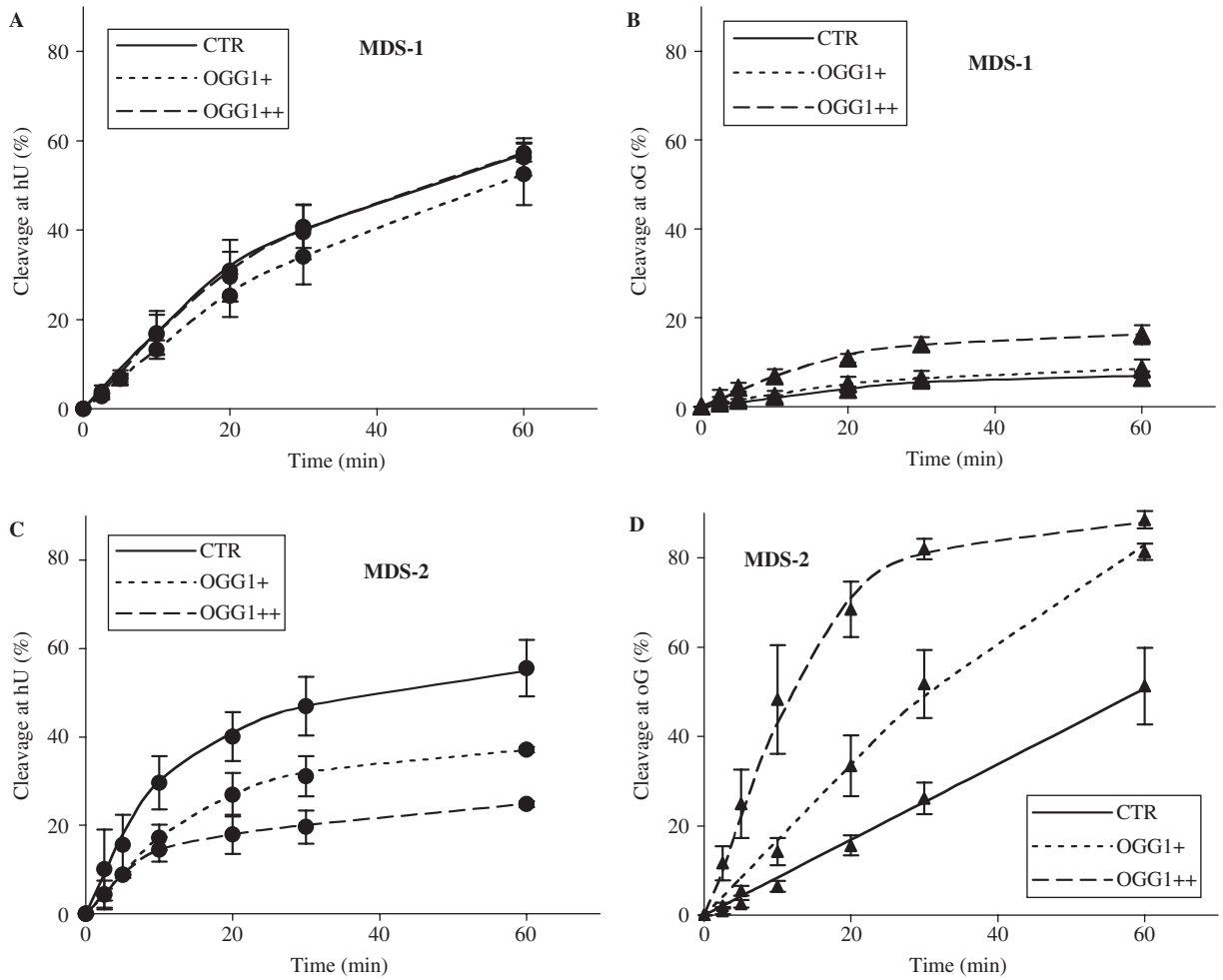

Figure 4. Excision efficiency at oG and hU on MDS-1 and MDS-2 by whole-cell extracts from hOGG1-overexpressing cells. DNA duplexes (1.5 pmol), were incubated with cell extracts (150 µg) for various time at 37°C and separated on a 12% denaturing polyacrylamide gel. Graphical representation of excision efficiency at hU (**A** and **C**) and oG (**B** and **D**) within MDS-1 (upper panels) or MDS-2 (lower panels) is shown as a function of the level of hOGG1 overexpression. Errors bars represent standard deviation from at least three independent experiments.

generated after hU cleavage was revealed (Figure 5, lane 10). This band virtually disappeared in the OGG1+ and OGG1++ cell extracts (lanes 11–12), while intensity of the band corresponding to the 7-nt fragment released after cleavage at oG rised proportionally. Then, to discriminate whether or not DSB were produced by cleavage at oG and hU on the same molecule, the duplex labeled on the strand carrying hU was used (Figure 5, lanes 13–16). Incubation of MDS-2 with CTR extracts led to the formation of two cleavage products correlating with DSB formation (Figure 5, lane 13). The 27 bp duplex corresponding to excision at hU represented 38% of the reaction products and the 23 bp duplex resulting from cleavage at hU and oG accounted for 17%. Overexpression of hOGG1 led to a major decrease of DSB formation, as revealed by the increased intensity of the band at 56 bp (intact substrate) with increasing hOGG1 level and by disappearance of the 27 bp DNA fragment (37 and 25% of cleavage leading to DSB formation in OGG1+ and OGG1++ extracts, respectively, versus 55% in CTR extracts, see lanes 14–16). This can be explained by the fact that, upon cleavage at oG and released of the 7-nt fragment (see lanes 10–12), hU is localized on a 9 nt single-stranded region. These results strongly suggested that in MDS-2, a DSB could be produced only if cleavage at hU occurred first, before that at oG. This is in fact in agreement with kinetics data shown in Figure 4C and D. To confirm this assumption, we engineered two DNA duplexes, named IMDS-hU/9 nt and IMDS-oG/DSB, to simulate repair intermediates formed by excision at oG or hU, respectively, from MDS-2 substrate. Cleavage at oG leaves hU that is situated on a 9 nt single-stranded region within the duplex (IMDS-hU/9 nt) and that cannot be further excised by cell extracts as shown in Figure 6A. In constrast, oG was very efficiently excised from IMDS-oG/DSB, when located at 3 nt from a DSB (Figure 6B). Therefore, hU is excised prior to oG when both damages are processed in MDS-2. Interestingly, cleavage at oG in IMDS-oG/DSB is facilitated in comparison with that in MDS-2 or SDS-oG (Figure 6C).

In conclusion, attempted repair of modified bases by normal cell extracts prevented DSB formation within

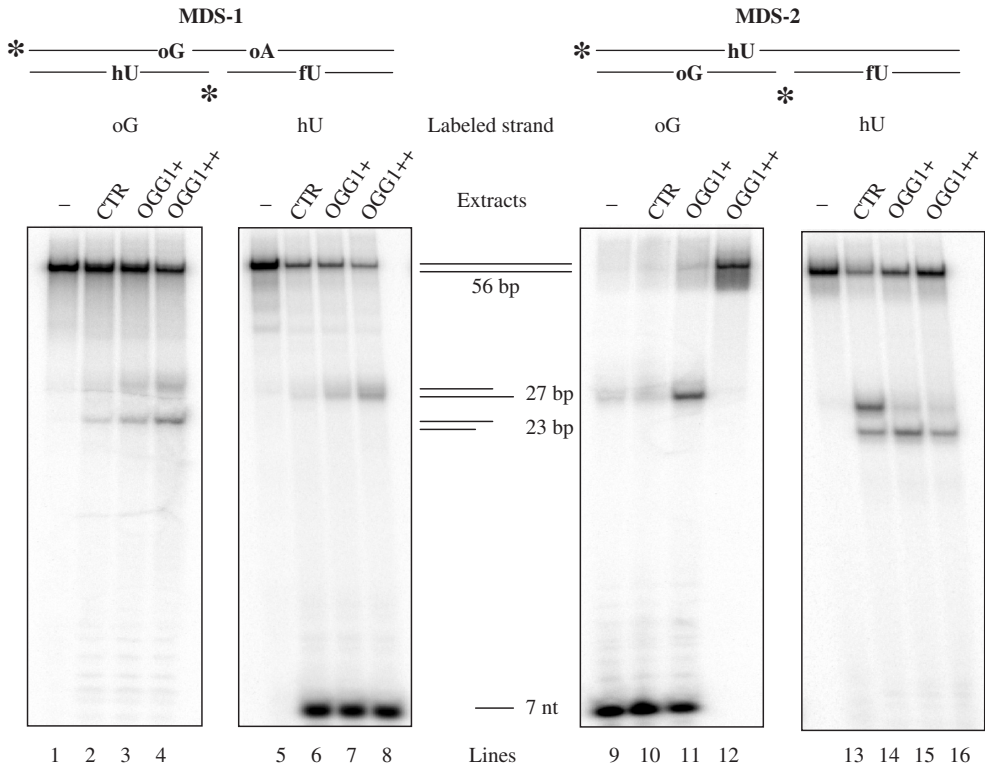

Figure 5. Double-strand break formation during the processing of MDS-1 and MDS-2 by extracts from hOGG1-overexpressing cells. DNA substrates (200 fmol), 5′-^{32}P-labeled on the oligonucleotide containing oG or hU as indicated in the figure, were allowed to react 1 h at 37°C with 20 μg of cell extracts from cells overexpressing or not hOGG1, and then subjected to native 12% polyacrylamide gel electrophoresis. Schematic representation of the labeled reaction products is shown in the center of the figure. Those duplexes comprise, respectively, 27 and 23 bp plus 4 protruding nucleotide. The substrates MDS-1 and MDS-2 were depicted on the top of the gels. Asterisks represent sites of phosphorylation.

MDS-1, whereas it did generate DSB within MDS-2. Moreover, the initial DSB formation in MDS-2 is likely to be followed by the lost of a 7 nt fragment, particularly in the presence of an excess of OGG1 protein. Taken together, these results demonstrate that the distribution of DNA damages and the level of the different DNA *N*-glycosylases/lyases available in cells determine the extent of DSB formation within a complex MDS, which may be accompanied by loss of genetic material.

DISCUSSION

This study assessed parameters that affect the repair of base damage within MDS. We previously provided evidence that there is a hierarchy in the incision efficiency at base damage within complex MDS and that this phenomenon prevents the formation of DSB as repair intermediate. We wished to further investigate on the parameters that controls this hierarchy. Indeed, one can expect that the first repair event occurring at a complex MDS is crucial for the fate and the biological consequences of those clustered lesions. We focused here on the initial incision rate at oG and hU by CHO cell extracts in two complex MDS carrying also a 1-nt gap at 4 bp on the opposite strand and other base damage nearby which are poorly (fU) or not (oA) excised (18).

It is shown that the efficiency of cleavage at oG is strongly sensitive to the environment. This may not be so surprising since OGG1 protein, the major DNA *N*-glycosylase/lyase in charge of removing oG in mammalian cells, interacts with the DNA backbone on 3′ and 5′ of oG and with the C paired with oG (33). The local DNA conformation should thus play an important role. The presence of the 1-nt gap likely introduces a kink in the duplex. An angle distribution value of ≈122° has been observed at a unique nick located at the center of a 139 bp DNA duplex and the angle distribution may result from an equilibrium between a stacked and a very flexible unstacked form (34). The presence of oxidized bases nearby may further weaken hydrogen bounds and base stacking interactions and displace the equilibrium towards the unstacked form. If a 1-nt gap opposite oG drastically reduces the hOGG1 binding at oG and its excision (Figure 2D, 15,18), it has no effect when located at 7 bp on the same strand (Figures 2B and 6C). The presence of base damage nearby (in IMDS-oG/hU) slightly inhibits cleavage efficiency at oG (Figure 6C and 18). Noteworthy, a DSB at 3 bp situated on the 5′ side of oG induces a favorable structure for interaction with OGG1 since oG is about 2 times more efficiently cleaved in IMDS-oG/DSB than as a single lesion (Figure 6C). The protein OGG1 interacts with 3 phosphates on the 3′ side of oG and with

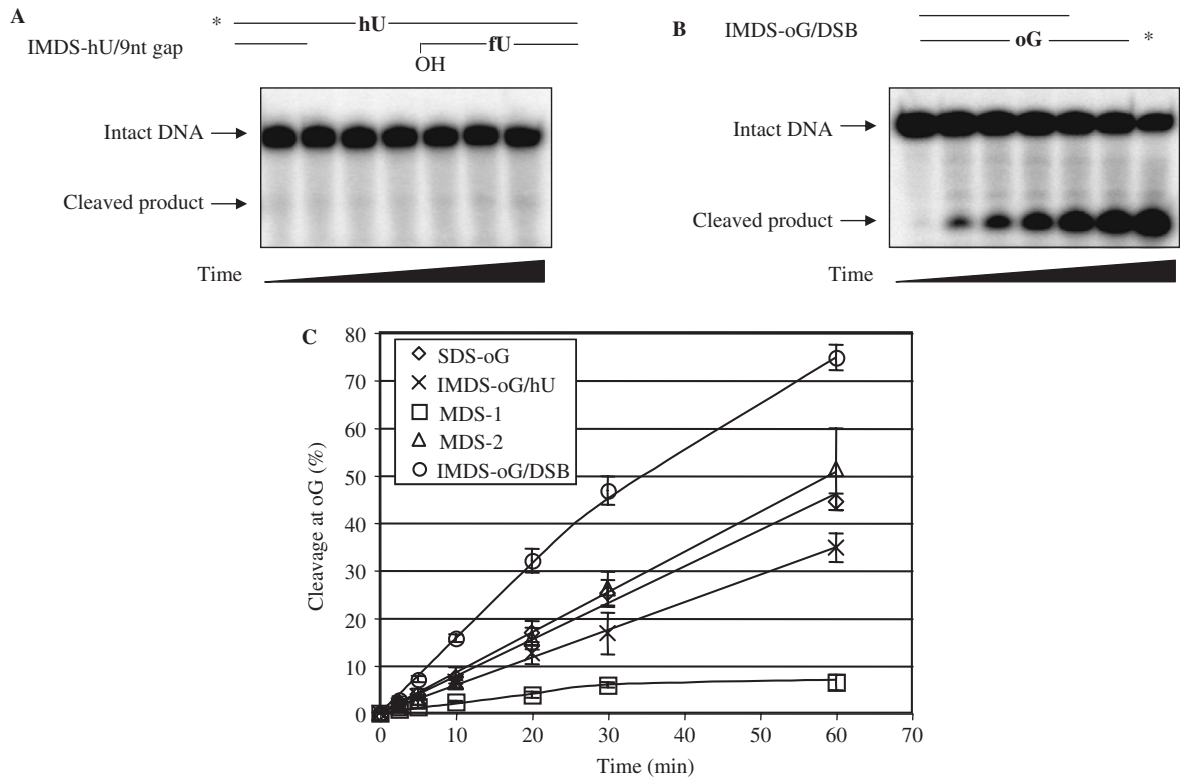

Figure 6. Efficiency of base excision on repair intermediates by CHO cell extracts. Reactions were performed on 5′-end labeled substrates as described in Material and Methods section. (**A**) Absence of cleavage at hU located in a single-stranded fragment in IMDS-hU/9 nt gap. (**B**) Efficient cleavage of IMDS-oG/DSB at oG by cell extract. In A and B the stars show the 5′-labeled ends. (**C**) Relative cleavage efficiency at oG in MDS of various complexity, including repair intermediates.

only one on the 5′ side (33). In addition, the binding of OGG1 protein at oG gives rise to a sharp bending (~70°) in the double helix, which may be energetically favored when oG is near an extremity of a DNA duplex. An alternative explanation would be an incision at oG by NEIL1 protein in IMDS-oG/DSB (35), but this is unlikely due to the increased oG removal by OGG1+ and OGG1++ extracts. Surprisingly, the proteins which cleave at hU, presumably NTH1, NEIL1 or MUG (30,36), are rather insensitive to the presence of damage nearby, including a 1 nt gap at 3 bp on the opposite strand and hU is as efficiently excised as unique lesion or within MDS (Figure 2C). The 1 nt gap in MDS-2 has no effect on cleavage at hU by the bacterial Nth (unpublished data). Meanwhile, a strong inhibitory effect on the efficiency of dihydrothymine excision by the bacterial Nth protein, due to the presence of an AP site 1–5 nt on the 5′ side on the complementary strand has been observed, as well as on excision by CHO XRS5 extracts (14). These observations may suggest that the protein, which binds to hU in MDS-2 takes advantage of the flexibility introduced by the 1-nt gap to accommodate the damaged base as in SDS-hU. Such an influence of local DNA structure on repair has already been reported for AP sites (37). Although, all these *N*-glycosylases bind to the base lesion and catalyze the flipping of the damaged deoxyribonucleotide into the active site, the unique property of OGG1 to interact with the opposed C provides a restricted substrate specificity and a great sensitivity to local DNA structure.

A major finding, which may be related to the above observation, is that the competition between DNA *N*-glycosylases at MDS of increasing complexity is always in favor of that (those) involved in the removal of oxidized pyrimidines, at least in the various contexts investigated here. Indeed, the initial incision rate at hU by extract from CHO cells (this study) and from human MRC5 cells (data not shown) is higher than at oG whatever the context tested, including single lesion (Figure 2E). Even though a small fraction of AP sites generated by OGG1 may not be cleaved, due to the low activity of APE/HAP1 under our conditions (absence of Mg), OGG1 *N*-glycosylase activity should still be activated by this last protein (38). In addition, previous work demonstrated that oG excision repair was poor and that the repair rate of oG/C by human and Chinese hamster cell extract was, respectively, 5 and 3-fold lower than that of U/A that, in turn, was repaired 10 and 3 times less efficiently than single abasic site (39). Such differences in repair rates only partly depended on levels of initiating enzymes, i.e. hOGG1, UNG or APE/HAP1 (40). The proteins in charge of oxidized/reduced pyrimidine may have higher affinity and activity than OGG1 for their respective substrates. The uncoupling of OGG1 *N*-glycosylase and AP lyase activities may slow down rather than accelerate

repair at oG. In support to our finding, a recent work suggests that, in *E. coli*, dihydrothymine may be excised prior to oG (41). It is probable that in mammalian cells, APE/HAP1 would be the first to make an incision at MDS carrying a free abasic site. This is supported by the high repair efficiency of abasic site within DNA clustered damage observed by Lomax *et al.* (42). Anyhow, our data demonstrate that the nature of base damage largely contributes to the base excision hierarchy within MDS and that excision efficiency partly depends on the damage distribution. Such findings are of importance to better predict the processing of various MDS and their biological consequences. Yet, whether base damage or SSB within MDS are repaired first is still an open question (18). Altogether, the above observations partly answer the question of who comes first at a complex MDS. They imply that, within MDS in cells, oxidized/reduced pyrimidine have better chance to be excised (and may be fully repaired) than oG, whereas the enhanced residency of oG is more prone to mutation induction.

Although factors like structural requirement, protein affinity and expression level may be evoked, the interplay between repair proteins, and in particular between DNA *N*-glycosylases, at MDS probably comprises some other features. We asked if the hierarchy in base excision that we observed and that can be now predicted, could be modulated or inverted. Our data bring the first evidence that base excision rate and hierarchy within complex MDS can be highly modified by overexpressing DNA *N*-glycosylases, i.e. OGG1 protein. We established a clone in CHO cells, here called OGG1++ that sufficiently overexpresses hOGG1 to exhibit a very high initial rate and final extent of incision at oG, as well as a higher DNA incision rate at oG than at hU as single lesions. Such a high level of hOGG1 protein within extract does not improve much the efficiency of oG excision in MDS-1 (Figure 4B), demonstrating the strong inhibitory effect of the 1-nt gap located at 3 bp on the opposite strand on the binding and/or the catalytic activity of hOGG1. In the MDS-1 configuration the fraction of DSB produced is very low and slightly increased in extracts from hOGG1-overexpressing cells. Importantly, the increased DSB production is accompanied by a loss of 9 nt, since a fraction of DSB results from cleavage at oG and hU (Figure 5). In addition, as a consequence of the efficient cleavage at hU that remains unchanged in hOGG1-overexpressing cell extract, the major product that results from the early steps in processing of MDS-1 is a 7 nt single stranded DNA fragment, leaving a majority of duplex with a 9-nt gap (Figure 5).

In contrast to MDS-1, the high level of hOGG1 allows an inversion of the excision hierarchy between oG and hU in MDS-2 (Figure 4C and D). Interestingly, it also strongly lowers the excision rate at hU in MDS-2 (Figure 4C). Consequently, DSB which are readily formed in normal extract (above 50% of reaction products), significantly diminish and are mainly accompanied by loss of genetic material resulting from cleavage at hU and oG. The increased incision rate at oG also leads to an enhanced release of the 7 nt single stranded piece and formation of duplex with a 9-nt gap (Figure 5). The hOGG1 overexpression is expected to have a more dramatic effect on the processing of the intermediary MDS which does not carry a 1-nt gap, namely IMDS-oG/hU (Figure 1). Indeed, initial rate of oG excision by OGG1++ extract is about 2-fold higher than hU excision, leading to a neat increase in DSB formation (37% of reaction products versus 14% for CTR extract, see Supplementary Data). We show here that hOGG1 overexpression does not necessarily lead to an inversion in base excision hierarchy within complex MDS, if oG is opposed to a SSB or a gap. Depending on damage distribution, it can result in different repair intermediates that lead to either an increase or a decrease of DSB associated with loss of a few nucleotides. It is most effective, in term of DSB formation, on clustered lesions containing only two opposed damaged base, i.e. oG and oxidized pyrimidine.

DNA damage induced by ionizing radiation comprise a significant proportion of clustered lesion, here called MDS. Human lymphoblastoid TK6 cells overexpressing hOGG1 or hNTH1 were shown to be slightly more sensitive to the toxic effect of γ-rays, and more sensitive to their mutagenic effect than control cells, whereas down-regulation of hOGG1 resulted in a reduced radiosensitivity (27,28). In addition, overexpression of either DNA *N*-glycosylase led to a significant increase in DSB post-irradiation, part of them were not resealed after 6 h. Likewise, we observed an enhanced mutation frequency induced by γ-rays with no increased toxicity in CHO cells that overexpress hOGG1, as compared to control cells (Figure 3C and D). As emphasized in (27), it is probable that in these cells, OGG1 protein in excess converts clustered lesions into mutagenic repair intermediates. Such biological data are indeed in good agreement with our biochemical observations based on model MDS. Indeed, in the case of complex MDS, possible but limited increase in DSB formed with nucleotides loss, is expected. Those DSB cannot be simply resealed in an error-free manner (by XRCC4/ligase IV for example) and would be either mutagenic or toxic. The rise in DSB formation observed in (27) rather results from cleavage at clustered lesions composed of two base damage including oG, similar to our IMDS-oG/hU. Some of these breaks may be quickly rejoined by core proteins of non-homologous end joining pathway, with or without mutations. Others, with «dirty» ends, may take longer to get repaired, presumably in an error-prone manner. The extensive formation of single stranded short region carrying base damage within DNA double helix observed with both complex MDS (increased by hOGG1 overexpression for MDS-2) should be highly mutagenic. Even though our model MDS may not be exactly those produced by γ-rays, our study bring further insight into the formation and the processing of MDS induced by ionizing radiation.

In summary, using more complex MDS than those composed of two lesions analyzed in the literature, we were able to demonstrate a hierarchy in the base excision within MDS, which mainly depends on the nature of the base damage (oxidized pyrimidine or purine) and may be modulated by the level of *N*-glycosylase/lyases. The base excision efficiency depends on damage distribution and

structural features at the MDS. Our studies plus others defined a number of parameters to get insight into the initial steps of repair at MDS and that allow to better predict the processing and the fate of MDS in cells. The excision hierarchy and repair inhibition occurring at MDS prevent an extensive formation of DSB, and thus, MDS should not induce drastic cell killing. In contrast, it favors the generation of short single stranded region carrying unrepaired base damage, later filled by repair synthesis, leading to point mutations. Our unpublished data on the processing of MDS in yeast *Saccharomyces cerevisiae* confirms such a scenario. The present study reinforces our previous hypothesis that MDS are more mutagenic than toxic lesions.

SUPPLEMENTARY DATA

Supplementary Data is available at NAR Online.

ACKNOWLEDGEMENTS

We are grateful to Dr P. Radicella (CNRS/CEA) for gift of repair enzymes, plasmid pPR65, hOGG1 antibodies and for helpful discussions. We thank Dr P.M. Girard (CNRS/Institut Curie, Orsay, France) for critical reading of the manuscript. This work was supported by Centre National de la Recherche Scientifique (CNRS), Institut Curie, Centre National d'Etudes Spatiales (CNES), Electricité de France (EDF). G. Eot-Houllier, M. Gonera and C. Giustranti were recipient of a doctoral fellowship from Ministère de l'Education Nationale, de la Recherche, et de la Technologie. G. Eot-Houllier and M. Gonera were recipient of a fellowship from Association pour la Recherche sur le Cancer. Funding to pay the Open Access publication charges for this article was provided by CNRS.

REFERENCES

1. Wallace, S.S. (1998) Enzymatic processing of radiation-induced free radical damage in DNA. *Radiat. Res.*, **150**, S60–S79.
2. Slupphaug, G., Kavli, B. and Krokan, H.E. (2003) The interacting pathways for prevention and repair of oxidative DNA damage. *Mutat. Res.*, **531**, 231–251.
3. Nikjoo, H., O'Neill, P., Terrissol, M. and Goodhead, D.T. (1994) Modelling of radiation-induced DNA damage: the early physical and chemical event. *Int. J. Radiat. Biol.*, **66**, 453–457.
4. Nikjoo, H., O'Neill, P., Wilson, W.E. and Goodhead, D.T. (2001) Computational approach for determining the spectrum of DNA damage induced by ionizing radiation. *Radiat. Res.*, **156**, 577–583.
5. Ward, J.F. (1988) DNA damage produced by ionizing radiation in mammalian cells: identities, mechanisms of formation, and reparability. *Prog. Nucleic Acid Res. Mol. Biol.*, **35**, 95–125.
6. Gulston, M., Fulford, J., Jenner, T., de Lara, C. and O'Neill, P. (2002) Clustered DNA damage induced by gamma radiation in human fibroblasts (HF19), hamster (V79-4) cells and plasmid DNA is revealed as Fpg and Nth sensitive sites. *Nucleic Acids Res.*, **30**, 3464–3472.
7. Sutherland, B.M., Bennett, P.V., Sutherland, J.C. and Laval, J. (2002) Clustered DNA damages induced by x rays in human cells. *Radiat. Res.*, **157**, 611–616.
8. Blaisdell, J.O., Harrison, L. and Wallace, S.S. (2001) Base excision repair processing of radiation-induced clustered DNA lesions. *Radiat. Prot. Dosimetry*, **97**, 25–31.
9. Weinfeld, M., Rasouli-Nia, A., Chaudhry, M.A. and Britten, R.A. (2001) Response of base excision repair enzymes to complex DNA lesions. *Radiat. Res.*, **156**, 584–589.
10. Chaudhry, M.A. and Weinfeld, M. (1995) The action of *Escherichia coli* endonuclease III on multiply damaged sites in DNA. *J. Mol. Biol.*, **249**, 914–922.
11. Chaudhry, M.A. and Weinfeld, M. (1997) Reactivity of human apurinic/apyrimidinic endonuclease and *Escherichia coli* exonuclease III with bistranded abasic sites in DNA. *J. Biol. Chem.*, **272**, 15650–15655.
12. Harrison, L., Hatahet, Z., Purmal, A.A. and Wallace, S.S. (1998) Multiply damaged sites in DNA: interactions with *Escherichia coli* endonucleases III and VIII. *Nucleic Acids Res.*, **26**, 932–941.
13. Harrison, L., Hatahet, Z. and Wallace, S.S. (1999) In vitro repair of synthetic ionizing radiation-induced multiply damaged DNA sites. *J. Mol. Biol.*, **290**, 667–684.
14. David-Cordonnier, M.H., Laval, J. and O'Neill, P. (2000) Clustered DNA damage, influence on damage excision by XRS5 nuclear extracts and *Escherichia coli* Nth and Fpg proteins. *J. Biol. Chem.*, **275**, 11865–11873.
15. David-Cordonnier, M.H., Boiteux, S. and O'Neill, P. (2001) Efficiency of excision of 8-oxo-guanine within DNA clustered damage by XRS5 nuclear extracts and purified human OGG1 protein. *Biochemistry*, **40**, 11811–11818.
16. David-Cordonnier, M.H., Cunniffe, S.M., Hickson, I.D. and O'Neill, P. (2002) Efficiency of incision of an AP site within clustered DNA damage by the major human AP endonuclease. *Biochemistry*, **41**, 634–642.
17. Lomax, M.E., Cunniffe, S. and O'Neill, P. (2004) 8-OxoG retards the activity of the ligase III/XRCC1 complex during the repair of a single-strand break, when present within a clustered DNA damage site. *DNA Repair (Amst)*, **3**, 289–299.
18. Eot-Houllier, G., Eon-Marchais, S., Gasparutto, D. and Sage, E. (2005) Processing of a complex multiply damaged DNA site by human cell extracts and purified repair proteins. *Nucleic Acids Res.*, **33**, 260–271.
19. Parsons, J.L., Dianova, I.I. and Dianov, G.L. (2005) APE1-dependent repair of DNA single-strand breaks containing 3′-end 8-oxoguanine. *Nucleic Acids Res.*, **33**, 2204–2209.
20. Dianov, G.L., Timchenko, T.V., Sinitsina, O.I., Kuzminov, A.V., Medvedev, O.A. and Salganik, R.I. (1991) Repair of uracil residues closely spaced on the opposite strands of plasmid DNA results in double-strand break and deletion formation. *Mol. Gen. Genet.*, **225**, 448–452.
21. Malyarchuk, S., Youngblood, R., Landry, A.M., Quillin, E. and Harrison, L. (2003) The mutation frequency of 8-oxo-7,8-dihydroguanine (8-oxodG) situated in a multiply damaged site: comparison of a single and two closely opposed 8-oxodG in *Escherichia coli*. *DNA Repair (Amst)*, **2**, 695–705.
22. Pearson, C.G., Shikazono, N., Thacker, J. and O'Neill, P. (2004) Enhanced mutagenic potential of 8-oxo-7,8-dihydroguanine when present within a clustered DNA damage site. *Nucleic Acids Res.*, **32**, 263–270.
23. D'Souza, D.I. and Harrison, L. (2003) Repair of clustered uracil DNA damages in *Escherichia coli*. *Nucleic Acids Res.*, **31**, 4573–4581.
24. Malyarchuk, S and Harrison, L. (2005) DNA repair of clustered uracils in HeLa cells. *J. Mol. Biol.*, **345**, 731–743.
25. Malyarchuk, S., Brame, K.L., Youngblood, R., Shi, R. and Harrison, L. (2004) Two clustered 8-oxo-7,8-dihydroguanine (8-oxodG) lesions increase the point mutation frequency of 8-oxodG, but do not result in double strand breaks or deletions in *Escherichia coli*. *Nucleic Acids Res.*, **32**, 5721–5731.
26. Blaisdell, J.O. and Wallace, S.S. (2002) Abortive base-excision repair of radiation-induced clustered DNA lesions in *Escherichia coli*. *Proc. Natl Acad. Sci. USA*, **98**, 7426–7430.
27. Yang, N., Galick, H. and Wallace, S.S. (2004) Attempted base excision repair of ionizing radiation damage in human lymphoblastoid cells produces lethal and mutagenic double strand breaks. *DNA Repair (Amst)*, **3**, 1323–1334.
28. Yang, N., Chaudhry, M.A. and Wallace, S.S. (2006) Base excision repair by hNTH1 and hOGG1: a two edged sword in the processing of DNA damage in γ-irradiated human cells. *DNA Repair (Amst)*, **5**, 43–51.

29. Hollenbach, S., Dhenaut, A., Eckert, I., Radicella, J.P. and Epe, B. (1999) Overexpression of Ogg1 in mammalian cells: effects on induced and spontaneous oxidative DNA damage and mutagenesis. *Carcinogenesis*, **20**, 1863–1868.
30. Ide, H. and Kotera, M. (2004) Human DNA glycosylases involved in the repair of oxidatively damaged DNA. *Biol. Pharm. Bull.*, **27**, 480–485.
31. Hazra, T.K., Kow, Y.W., Hatahet, Z., Imhoff, B., Boldogh, I., Mokkapati, S.K., Mitra, S. and Izumi, T. (2002) Identification and characterization of a novel human DNA glycosylase for repair of cytosine-derived lesions. *J. Biol. Chem.*, **277**, 30417–30420.
32. Gros, L., Ishchenko, A.A., Ide, H., Elder, R.H. and Saparbaev, M.K. (2004) The major human AP endonuclease (Ape1) is involved in the nucleotide incision repair pathway. *Nucleic Acids Res.*, **32**, 73–81.
33. Bruner, S.D., Norman, D.P. and Verdine, G.L. (2000) Structural basis for recognition and repair of the endogenous mutagen 8-oxoguanine in DNA. *Nature*, **403**, 859–866.
34. Le Cam, E., Fack, F., Ménissier-de Murcia, J., Cognet, J., Barbin, A., Sarantoglou, V., Révet, B., Delain, E. and de Murcia, G. (1994) Conformational analysis of a 139 base-pair DNA fragment containing a single-stranded break and its interaction with human Poly(ADP-ribose) polymerase. *J. Mol. Biol.*, **235**, 1062–1071.
35. Parsons, J.L., Zarkhov, D. and Dianov, G.L. (2005) NEIL1 excises 3′ end proximal oxidative DNA lesions resistant to cleavage by NTH1 and OGG1. *Nucleic Acids Res.*, **33**, 4849–4856.
36. Kow, Y.W. (2002) Repair of deaminated bases in DNA. *Free Radic. Biol. Med.*, **33**, 886–893.
37. Lin, Z. and de los Santos, C. (2001) NMR characterization of clustered bistrand abasic site lesions: effect of orientation on their solution structure. *J. Mol. Biol.*, **308**, 341–352.
38. Vidal, A.E., Hickson, I.D., Boiteux, S. and Radicella, J.P. (2001) Mechanism of stimulation of the DNA glycosylase activity of hOGG1 by the major human AP endonuclease: bypass of the AP lyase activity step. *Nucleic Acids Res.*, **29**, 1285–1292.
39. Cappelli, E., Degan, P. and Frosina, G. (2000) Comparative repair of the endogenous lesions 8-oxo-7, 8-dihydroguanine (8-oxoG), uracil and abasic site by mammalian cell extracts: 8-oxoG is poorly repaired by human cell extracts. *Carcinogenesis*, **21**, 1135–1141.
40. Cappelli, E., Hazra, T., Hill, J.W., Slupphaug, G., Bogliolo, M. and Frosina, G. (2001) Rates of base excision repair are not solely dependent on levels of initiating enzymes. *Carcinogenesis*, **22**, 387–393.
41. Shikazono, N., Pearson, C., O'Neill, P. and Thacker, J. (2006) The roles of specific glycosylases in determining the mutagenic consequences of clustered DNA base damage. *Nucleic Acids Res.*, **34**, 3722–3730.
42. Lomax, M.E., Cunniffe, S. and O'Neill, P. (2004) Efficiency of repair of an abasic site within DNA clustered damage sites by mammalian cell nuclear extracts. *Biochemistry*, **43**, 11017–11026.